ECI 8th International Conference on Boiling and Condensation Heat Transfer
Ecole Polytechnique Fédérale de Lausanne, 3-7 June 2012
Lausanne, Switzerland

PERFORMANCE OF TWO-PHASE CONFINED IMPINGING SUBCOOLED WATER JETS

Michael Sabo, Christopher Stull, Deborah Pence* and James Liburdy
*Author for correspondence
Mechanical Engineering
Oregon State University
Corvallis, OR 97331-6001 USA
E-mail: Deborah.Pence@Oregonstate.edu

ABSTRACT

Advances in electronics fabrication, coupled with the demand for increased computing power, have driven research into innovative cooling solutions to dissipate heat from these devices. To meet future demands, previous research has focused on robust and stable two-phase heat sinks. In the present study, a confined, subcooled impinging jet is explored as means of achieving two-phase heat transfer while leveraging an increase in flow area to minimize flow instabilities frequently observed in standard microchannel heat sinks.

The test device consists of a 4 mm diameter jet of 10°C subcooled water impinging on a 38 mm diameter heated aluminum surface. The exit of the confined jet is submerged. Experimental parameters include jet Reynolds numbers between 2500 and 10,000, nondimensional gap spacing between 0.25 and 2, and input heat fluxes between 0 and 90 W/cm^2. The influence of these parameters on heat transfer performance is assessed.

The experimental facility was validated by conducting tests in absence of the jet, when the impingement surface was subjected to pool boiling. Boiling curves acquired using the confined impinging jet configuration include single-phase transfer, the results of which are influenced by heat flux, but not by the confinement spacing. Over the range of conditions tested, pressure drops across the jet were imperceptibly small, yielding an efficient means of removing significant amounts of heat while operating in an inherently stable manner. An existing correlation derived from confined impinging jets with two-phase inlet conditions was modified for the present conditions. Preliminary studies conducted with in-situ vapor extraction, by replacing the impermeable confinement surface with one that is porous and subjected to a vacuum, suggest the potential for heat transfer enhancement by reduction of the quality within the experimental device.

INTRODUCTION

Several studies particularly relevant to the present study are highlighted. Presented first are studies conducted using confined, submerged, single-phase impinging jets. Then, based on an assessment of current high heat flux cooling technologies presented by Mudawar (2001), impinging jet studies conducted with phase change are highlighted. In the context of impinging jet heat transfer, the nucleate boiling literature is presented under four general categories: jet velocity, subcooling, nozzle and heater dimensions, and nozzle-to-surface spacing.

Stagnation point Nusselt numbers and local averaged Nusselt numbers were studied by Chang et al (1995a) as a function of jet Reynolds number and nozzle-to-surface spacing (gap height) for a single-phase, confined and submerged jet. Refrigerant R-113 was used as the working fluid. Heat transfer data show a slight decrease in the stagnation Nusselt number for gap heights less than the length of the potential core, as would be defined for an unconfined jet flow. The decrease is attributed to a recirculation vortex, which caused the emerging jet to break up prematurely. The degree to which the recirculating vortex influences heat transfer is dependent upon vortex size and vortex intensity, both of which are dependent on the gap height and inertia of the impinging jet.

Garimella and Rice (1995) used laser-Doppler velocimetry to examine recirculation zones in a confined, liquid impinging jet of FC-77 with nozzle diameters of 6.35 mm and 3.18 mm, nondimensional gap height, H/d_j, of 2, 3 and 4, and jet Reynolds numbers of 8500, 13,000 and 23,000. Recirculation zones were found to be a function of both gap height and Reynolds number. The center of the vortex moved radially outwards with increases in Reynolds number, *Re*, and with increases in gap spacing, whereas secondary peaks in local heat transfer coefficients became more pronounced at smaller gap spacing.

Later, Garimella and Nenaydykh (1996) assessed the influence of nozzle geometries on confined liquid jet impingement heat transfer. Using nozzles with different diameters and different aspect ratios, defined as the nozzle length divided by nozzle diameter, L/d_j, the effects of flow development and separation on the heat transfer coefficient were examined. For very small aspect ratios, below unity, heat transfer coefficients were at a maximum. For aspect ratios between 1 and 4, a sharp decrease in the heat transfer coefficient was observed. For aspect ratios between 4 and 8, the heat transfer coefficient gradually increased.

The cause of these trends was attributed to flow separation and reattachment inside the nozzle and its consequential influence on the exit velocity profile. An increase in the nozzle diameter showed a substantial increase in the stagnation heat transfer coefficient, for a fixed *Re*, L/d_j, and H/d_j. Turbulence intensity near the jet centerline was higher for larger jet diameters and postulated as the reason for observed increases in the stagnation heat transfer coefficient.

Li and Garimella (2001) studied the influence of thermophysical properties on heat transfer in confined liquid impinging jets. Air, water and FC-77 were employed as working fluids. Correlations were developed for the stagnation and area-averaged Nusselt numbers as a function of the *Re*, Prandtl number, L/d_j, and the ratio of impingement surface diameter to nozzle diameter. In the correlations, the exponent for Prandtl number, *Pr*, was experimentally determined to be 0.441 instead of constraining the value to 0.4, as in previous work.

Attention is now turned to two-phase heat transfer. For nucleate boiling conditions, the ratio of heat flux over surface temperature in a confined, submerged jet was shown to be relatively unaffected by jet velocity by Katto and Kunihiro (1973) and Kamata et al (1988) using water as the working fluid, by Mudawar and Wadsworth (1991) using FC-72 as the working fluid and by Zhou et al (2004) using R-113 as the working fluid. However, higher jet velocities were shown by Katto and Kunihiro (1973) to delay the incipience of nucleate boiling, a phenomenon confirmed by Ma and Bergles (1986) for a circular submerged jet of saturated R-113. Although heat transfer in the nucleate boiling regime, which is dominated by the intense mixing of vapor bubbles leaving the heated surface, is not influenced by convection heat transfer resulting directly from the jet velocity, jet velocity was found and reported in Wolf et al (1993) to influence both the sub-cooled and the partial boiling regimes. In all cases, boiling curves for confined, submerged jets show higher values of heat flux and surface temperature than achievable with pool boiling.

With increases in the degree of subcooling, Ma and Bergles (1986) report a delay in the incipience of nucleate boiling and a slight shift to the left of the nucleate boiling regime on the boiling curve. Mudawar and Wadsworth (1991) and Zhou et al (2004) in confined submerged jets, and Lui et al (2004) in a free surface jet also report a delay in the incipience of nucleate boiling with increases in subcooling; however, none observed a shift of the boiling curve in the nucleate boiling regime.

The relationship between heat flux and surface temperature in the nucleate boiling regime is insensitive to changes in jet nozzle diameter in a confined, submerged jet, as reported by Katto and Kunihiro (1973), Wadsworth (1990) using FC-72, and Monde and Katto (1978). Furthermore, the influence of gap height on the Nusselt number at the stagnation point under nucleate boiling heat transfer conditions was shown by Kamata et al (1988) and Monde and Katto (1977) to be insignificant.

Refrigerant-113 entering a confined and submerged jet in a two-phase liquid-vapor state was investigated by Chang et al (1995b) to determine the influence of Reynolds number, gap height, and inlet quality. Consistent with previous studies, changes in Reynolds number and gap height were found to yield negligible influence on the ratio of heat flux over surface temperature. However, the inlet quality of the jet was found to greatly enhance the local heat transfer coefficient, by as much as 100% throughout the confinement region. Inlet quality was taken into account in the heat transfer correlation developed in that study.

In summary, although single-phase heat transfer in a confined impinging jet is influenced by jet Reynolds number, gap height, subcooling and nozzle size, nucleate boiling heat transfer is relatively unaffected by these parameters. These parameters do, however, contribute to a delay in incipience of boiling and extension of the boiling curve to higher values of heat flux and excess temperature. The parameter with the greatest influence on nucleate boiling heat transfer appears to be inlet quality. With a base understanding of heat transfer in a subcooled, confined and submerged impinging jet developed for the present study, future studies of heat transfer with in-situ vapor extraction from the confinement region will be conducted.

EXPERIMENTAL TEST SETUP

Figure 1 provides a cross-section schematic representation of the confined, submerged impinging jet. Performance of the jet was assessed by varying the jet Reynolds number, Re_j, and non-dimensional gap height, H/d_j, according to the test matrix provided in Table 1 for a range of applied heat flux, q'' Held fixed were the subcooling, at 10°C, the jet diameter, at 4 mm, and the impingement surface diameter, at 38 mm. The heated surface was gold plated aluminum insulated with a two-piece PEEK manifold containing fluid interconnects, instrumentation ports, and viewing ports for control of the fluid height in the exit plenum. The gap height was set using precision gage blocks placed between the upper and lower manifold pieces. The aluminum block was heated using five 9.5 mm diameter, 300 W cartridge heaters. Three T-type thermocouples were embedded at different depths from the heated surface, offset at 5 mm intervals, and used to extrapolate surface temperatures.

Table 1 Experimental test matrix.

	Re_j		
H/d_j	2500	5000	10000
0.25	X	X	X
0.5	X	X	X
1	X	X	X
1.5	X	X	X
2	X	X	X

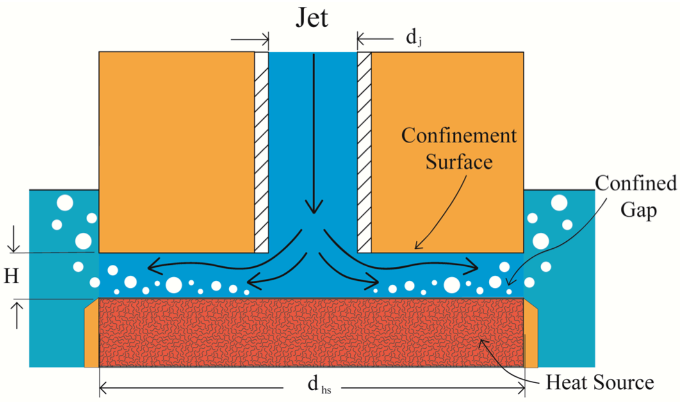

Figure 1 Cross-section of confined impinging jet.

A flow loop, shown in Figure 2, was designed to supply the working fluid, distilled and degassed water, to the test piece. A converted hot water heater serves as the degassing and storage tank for the distilled water. After degassing, the water is pumped, using a Micropump gear pump, through a series of filters and a needle valve for fine control over the flow rate. The inlet mass flow rate is measured using a MicroMotion Coriolis flow meter before entering the constant temperature oil bath used to preheat the water to a condition in which it enters the test piece at approximately 10°C below the saturation temperature. Fine-tuning of the inlet fluid temperature is achieved with rope heaters wrapped around the inlet ducting. Pressure and temperature measurements are collected directly upstream of the nozzle inlet as well as in the exit plenum, which is used to control the level to which the confined jet is submerged.

The generated vapor generated by the heated surface leaves through the top of the exit plenum, whereas excess liquid drains from the bottom. Vapor flows through a condenser prior to the condensate being collected and recorded using a catch and weigh method. The liquid level in the exit plenum is controlled with a pump and needle valve located in the liquid drain line. A second MicroMotion Coriolis flow meter measures the exiting liquid mass flow rate prior to it returning to the degassing tank.

Pressure and temperature measurements are collected at several locations in the flow loop and test piece. In the test piece, threaded ports allow for pressure transducer taps and sheathed thermocouples installation using compression fittings. A piezo-resistive, absolute pressure transducer with a range of 0 to 206 kPa is located at the inlet of the nozzle using a T-fitting. A 0 to 103 kPa range differential pressure transducer is connected with one port to the inlet T-fitting and the second port to the outlet plenum. Thermocouples used for temperature measurements were shielded and grounded T-type. The device was tested for leaks prior to testing.

Bias and precision errors were estimated for each of the instruments. The error associated with the linear curve fit of the calibration data was found using the standard error estimate. The repeated measurement error is calculated from the data and propagated to the final calculated result using the Kline and McClintock method, as reported in Figliola and Beasley (1995). Uncertainties in heat flux of approximately 5.5 W/cm^2, or 6% of the maximum applied heat flux, are mainly a function of the input power. This uncertainty was consistent over the range of heat fluxes used for testing. The maximum calculated uncertainly for the excess temperature is approximately 1.5°C. Representative uncertainty values are shown as error bars in the figures. Additional information regarding the test facility and uncertainty estimates are provided in Sabo (2012).

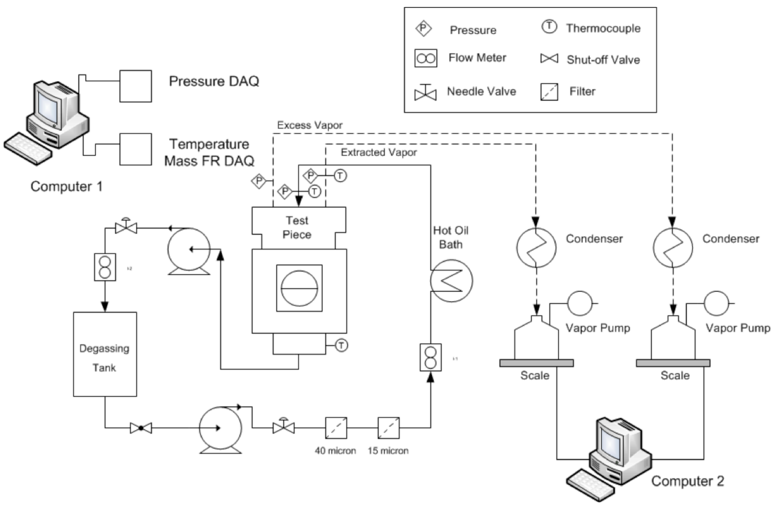

Figure 2 Experimental test facility.

ANALYSIS

The applied surface heat flux is calculated using

$$q''_s = \frac{IV - Q_{loss}}{A_s} \quad (1)$$

where Q_{loss} was determined from a heat loss experiment, I is the measured amperage, V is the measured voltage, and A_s is the heated impingement surface area. To assess heat loss during operation, the impingement surface was insulted with a one inch thick piece of Teflon® while 10°C sub-cooled water was circulated through the exit plenum of the device, the latter of which simulated operating conditions. Power was supplied in increments of 5 W and the resulting heater block temperature was recorded. A linear fit was applied to the data, yielding the following relation

$$Q_{loss} = 0.414(T_{HB}) - 35.2 \quad (2)$$

which relates heat loss to heater block temperature and has a standard error of the fit equal to 1.94 W. The wall temperature is extrapolated using a 1-D conduction analysis based on the surface heat flux from Equation (1) and middle thermocouple reading

$$T_w = T_{HB2} - \frac{q''_s}{k_{Al}\Delta_{2w}} \quad (3)$$

In Equation (3), T_{HB2} is the middle heater block temperature, k_{Al} is the thermal conductivity of the aluminum heater block, and Δ_{2w} is the distance from the thermocouple junction to the wall.

CORRELATIONS

Chang et al (1995a) developed a single-phase correlation for a confined, submerged impinging jet with R-113 as the working fluid. Spatially-averaged for a uniform wall temperature, the single-phase heat transfer coefficient is

$$\overline{h_{1\phi}}(r) = 0.7017\frac{k_l}{d_j}\mathrm{Re}_j^{0.574}\,\mathrm{Pr}^{0.4}\left(\frac{H}{d_j}\right)^{-0.106}\left(\frac{r}{d_j}\right)^{-0.62} \quad (4)$$

where r corresponds to the radial distance along the heated surface, measured from the point of impingement. Additionally, Chang et al (1995b) developed a two-phase confined jet correlation for R-113 that uses the principle of superposition to combine the contributions of the single-phase, $q''_{1\Phi}$, and nucleate boiling, q''_{NB}, heat transfer according to:

$$q''_{tot} = q''_{1\phi} + q''_{NB} \quad (5)$$

Using the appropriated driving temperature differences, Equation (5) can be rewritten as

$$q''_{tot} = \bar{h}_{1\phi}(T_w - T_b) + \bar{h}_{NB}(T_w - T_{sat}) \quad (6)$$

where T_w is the wall temperature, T_b is the bulk fluid temperature, and T_{sat} is the saturation temperature corresponding to the inlet pressure of the jet. The single-phase heat transfer coefficient is defined in Equation (4), whereas the nucleate boiling heat transfer coefficient, developed by Chang et al (1995b) with R-113 as the working fluid, is computed from

$$\bar{h}_{NB} = \mu_l i_{lv}\left[\frac{g(\rho_l - \rho_v)}{\sigma}\right]^{1/2}\left(\frac{c_{p,l}}{C_{s,f}\,i_{lv}\,\mathrm{Pr}_l^n}\right)^{3.5}\Delta T_e^{2.5} \quad (7)$$

Equation (7) is based on the pool boiling correlation from Rohsenow (1952)

$$q''_s = \mu_l i_{lv}\left[\frac{g(\rho_l - \rho_v)}{\sigma}\right]^{1/2}\left(\frac{c_{p,l}\Delta T_e}{C_{s,f}\,i_{lv}\,\mathrm{Pr}_l^n}\right)^{3} \quad (8)$$

which relates the excess temperature to the applied heat flux based on the properties of the working fluid and the heated surface. To adapt the correlation for use with the current experimental configuration, the constant $C_{s,f}$ and the exponent on the Prandtl number, n, were experimentally determined by comparing the Rohsenow (1952) correlation with data acquired using the heater block and lower housing of the test manifold subjected to pool boiling conditions.

RESULTS

In order to assess the influence of gap height and jet Reynolds number on heat transfer performance of the confined, submerged impinging jet, boiling curves were generated for each nominal test case reported in Table 1. Experimental data from the pool boiling experiment are reported in Figure 3, along with the pool boiling correlation from Rohsenhow (1952). The value

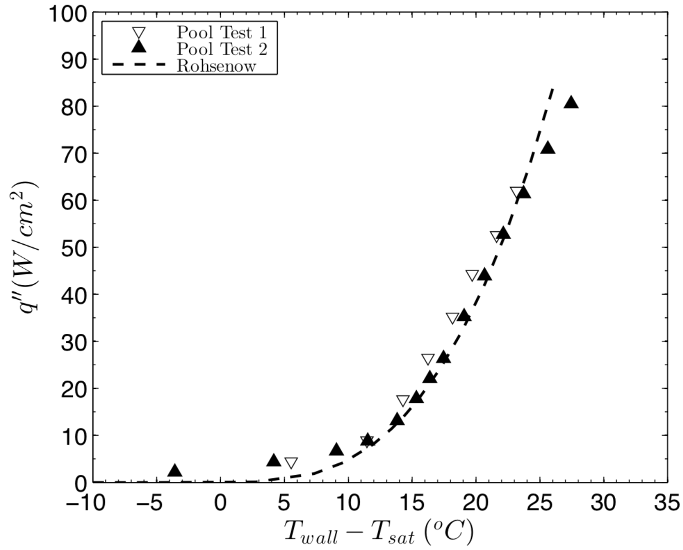

Figure 3 Comparison of pool boiling data to Rohsenow (1952) correlation.

used for the coefficient $C_{s,f}$ is 0.016 with the exponent n assigned a value of 1.26. These values are within the ranges reported by Pioro (1999) for a water/aluminum fluid-surface combination.

Figure 4 illustrates the influence of jet Reynolds number for a non-dimensional gap spacing of 1.5. Increases in jet Reynolds number serve to enhance heat transfer in the single-phase regime and delay the onset of nucleate boiling (ONB) over the range of test conditions examined. The ONB generally corresponds to the change in slope of the boiling curve. For example in Figure 4, ONB for the nominal Re_j case of 2500 appears to occur at an excess temperature of approximately 6°C, whereas the ONB is delayed to approximately 11°C for the nominal Re_j case of 10,000. These results agree with trends reported in the literature, including that of Wolf et al (1993). Once the onset of nucleate boiling occurs, the heat transfer is dominated by the formation and departure of bubbles on the heated surface. The latent energy exchange results in the increase in the slope of heat flux as a function of excess temperature. To validate that the changes in slope observed in Figure 4 do correspond with the onset of nucleate boiling, the heat flux necessary to heat the working fluid from the 10°C sub-cooled inlet condition to a saturated condition is estimated using

$$q''_{SB} = \frac{\dot{m}_{in}}{A_s}(i_{sat,l} - i_{in,l}) \tag{9}$$

where, $i_{in,l}$ is the enthalpy at the inlet evaluated using the inlet temperature and pressure, and $i_{sat,l}$ is the saturated liquid enthalpy evaluated using the inlet pressure. Heat flux values computed from Equation (9) are shown as horizontal lines in Figure 5. Heat

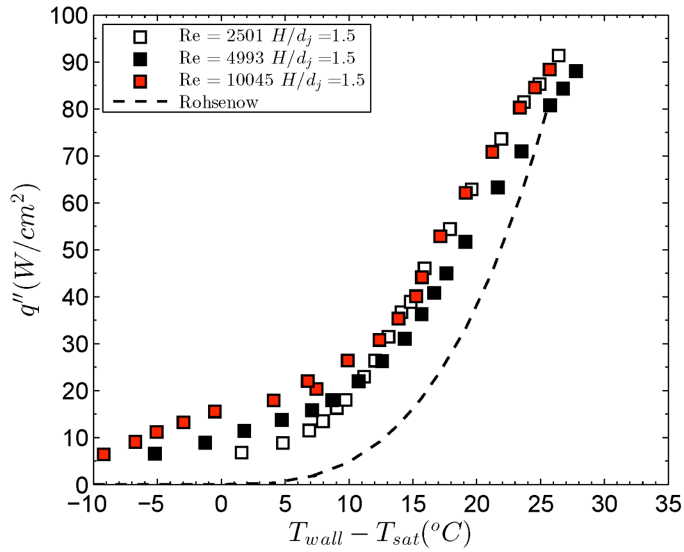

Figure 4 Influence of Reynolds number on performance shown with the Rohsenow (1952) correlation.

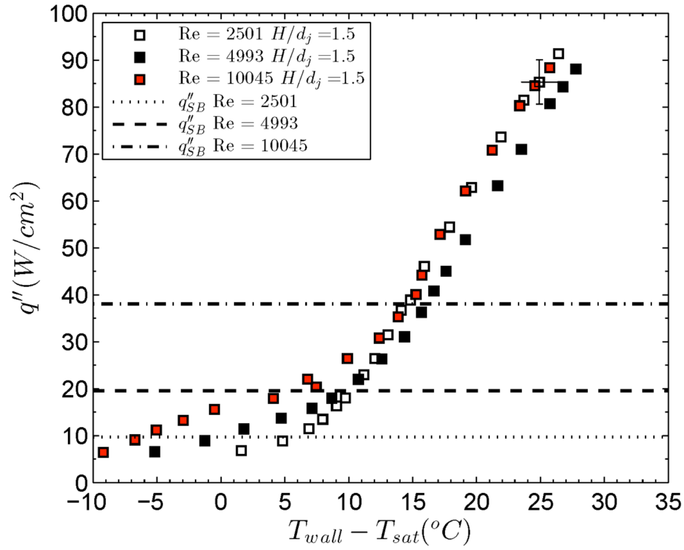

Figure 5 Calculated heat fluxes (horizontal lines) corresponding to the onset of nucleate boiling (changes in slope).

flux values correspond well with changes in slope of the boiling curve, thus confirming that the observed changes in slope correspond with the transition from single-phase to nucleate boiling heat transfer.

The influence of nondimensional gap height on the boiling curve is illustrated in Figure 6 for a nominal Re_j of 10,000. As expected there is little influence of gap height on the nucleate boiling regime. Although recirculation vortices, dependent upon the gap height, for single-phase flows were reported by Garimella and Rice (1995) to influence local temperature distributions, no influence is observed in the present data.

The influence of jet Reynolds number for a fixed nondimensional gap height of 0.5 is shown in Figure 7. Any observed differences in heat flux and excess wall temperature as a function of Re_j in the nucleate boiling regime are within the ranges of uncertainty. Trends of single-phase heat transfer are expected, demonstrating an increase with increases in Reynolds number. Also plotted on Figures 7, as a function of Re_j, are predicted heat fluxes computed from Equations (4), (6) and (7) using values of $C_{sf} = 0.016$ and $n = 1.26$, and using the measured impinging surface temperature, T_w, found from Equations (1) through (3).

Using ±25% error bands, the experimental versus calculated values of heat flux are plotted in Figure 8. For a nominal Re_j of 2500 and heat flux values less than 60 W/cm^2, the correlation under predicts experiments. For heat fluxes above 80 W/cm^2, predictions for all Re_j begin to breakdown. This can be attributed to the fact that the two-phase component of the heat transfer correlation was derived from the Rohsenow (1952) pool boiling correlation, which is valid only for the isolated bubble formation region of the boiling curve. Heat fluxes greater than 80 W/cm^2 are expected to correspond to the columns and jets region of the boiling curve. Overall, the Chang et al (1995b) correlation, modified to account for a sub-cooled inlet condition and using

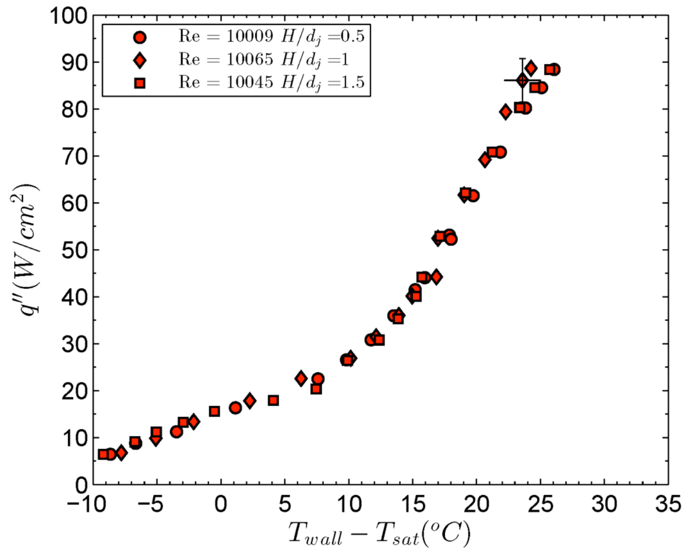

Figure 6 Influence of non-dimensional gap spacing on heat transfer performance.

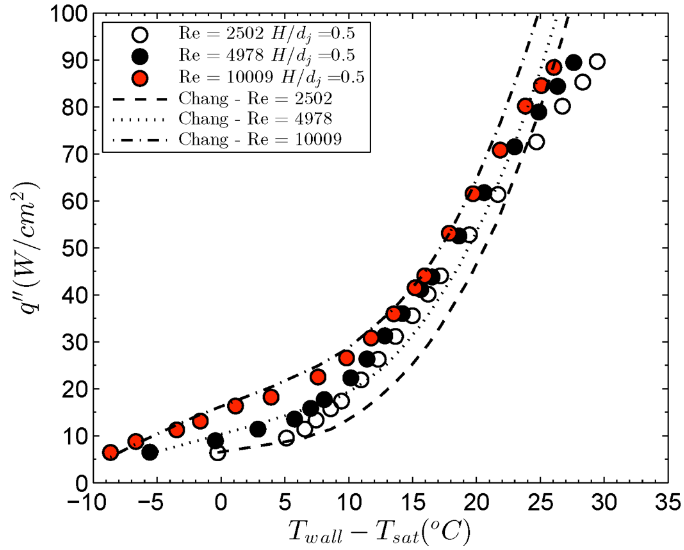

Figure 7 Comparison of experimental data to the two-phase jet correlation for an $H/d_j = 0.5$.

constants appropriate for current experimental conditions, is fairly successful at predicting the surface heat flux for the 5000 and 10,000 Reynolds number cases and heat flux values less than 80 W/cm^2.

Average inlet pressures for the three jet Reynolds numbers at a non-dimensional gap spacing of 1.5 are shown in Figure 9. The inlet pressure is relatively constant in the single-phase region. Once nucleate boiling begins, the inlet pressure drops slightly and then increases again as the rate at which vapor is generated begins to increase. Onset of nucleate boiling, calculated using Equation (9), is shown as vertical lines in Figure 9 and agrees well with the point at which the inlet pressure drops. The decrease in the inlet pressure results from the increased mixing of the fluid, due to the bubble formation and departure, which lowers the bulk viscosity of the fluid and overall pressure drop through the device. Given the exit pressure is fixed, a decrease in pressure drop corresponds to a decrease in inlet pressure. After the minimum in inlet pressure, the heat flux and corresponding vapour generation increases, as does the pressure drop. The heat flux corresponding to the drop in inlet pressure depends on mass flow rate, as this dictates when boiling occurs.

Preliminary boiling data were also acquired for conditions in which the confinement surface, originally impermeable, was changed to a porous surface consisting of a porous aluminium support block, having an average pore size of 15 μm and average porosity of 15%, and a hydrophobic, 0.22 μm pore Telfon® membrane in contact with the working fluid. The combined permeability was measured to be 2.64 e-14 m^2 ± 1.6 e-15 m^2. Details of the experimental test facility used for extraction studies are provided in Stull (2012). Applying a vacuum on the aluminium side of the porous confinement surface, vapour generated within the confined gap was extracted. The result is shown in Figure 10 as a shift in the nucleate boiling regime of the boiling curve. At an excess wall temperature of 20°C, there is a 20% increase in heat flux with extraction compared to that without. This

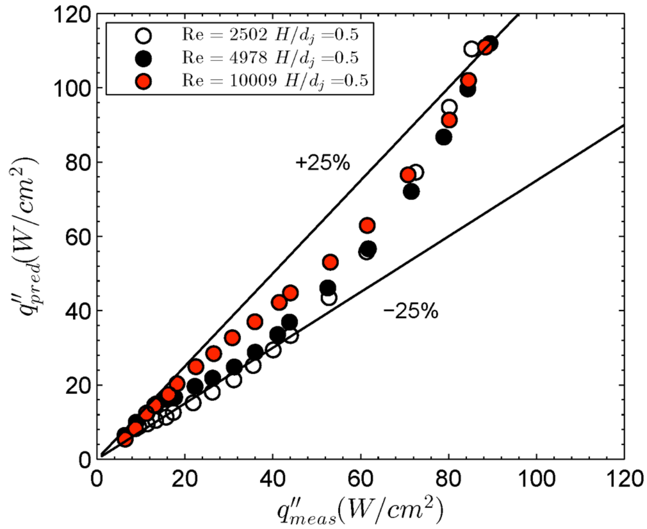

Figure 8 Comparison of experimental data to the two-phase jet correlation for an $H/d_j = 0.5$.

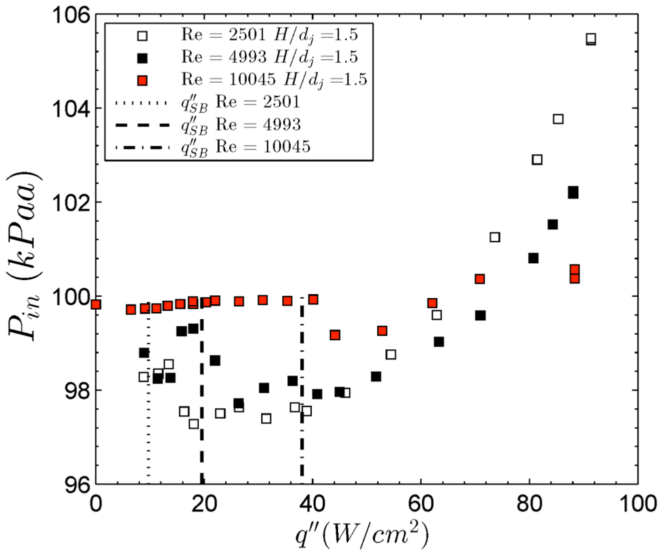

Figure 9 Inlet pressure as a function of heat flux for varying Reynolds numbers at an H/d_j = 0.5.

observed enhancement is consistent with the observation made by Chang et al (1995b), in the sense that changes in inlet quality, which yield a consequential change in quality throughout the confined jet, has the potential to influence the nucleate boiling regime of the boiling curve.

Presented in Figure 11 is the ratio of vapour extracted mass flow rate over the inlet mass flow rate, where the extracted mass flow rate is determined from

$$Q_{in} + \dot{m}_{in} i_{in,l} = \dot{m}_{ext} i_{ext} + \dot{m}_{out} i_{out} \tag{10}$$

In Equation (10), the outlet includes the liquid exiting the confined gas as well as any excess vapour not extracted. Also presented in Figure 11 is the exit quality with no extraction, determined from

$$\chi_{out} = \frac{i_{out} - i_l}{i_v - i_l} \tag{11}$$

as well as the exit quality with extraction

$$\chi_{out,ext} = \chi_{out} - \frac{\dot{m}_{ext}}{\dot{m}_{in}} \tag{12}$$

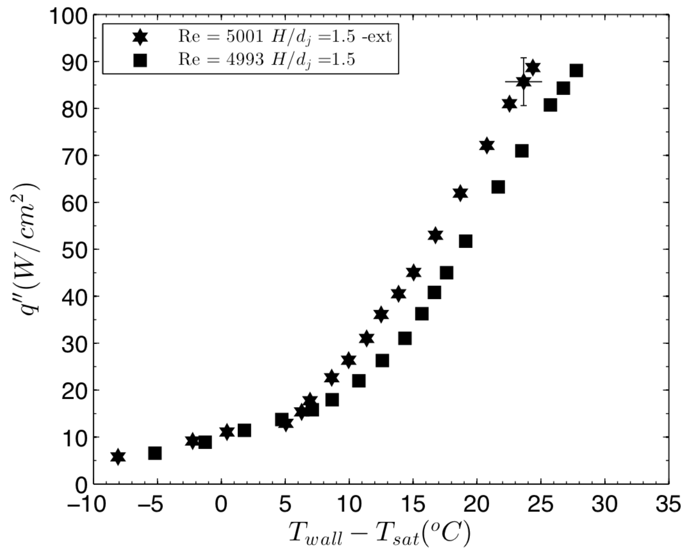

Figure 10 Comparison of boiling curves for Re = 5000, H/d_j =1.5 for a non-extraction and a 30 kPa (absolute) extraction pressure.

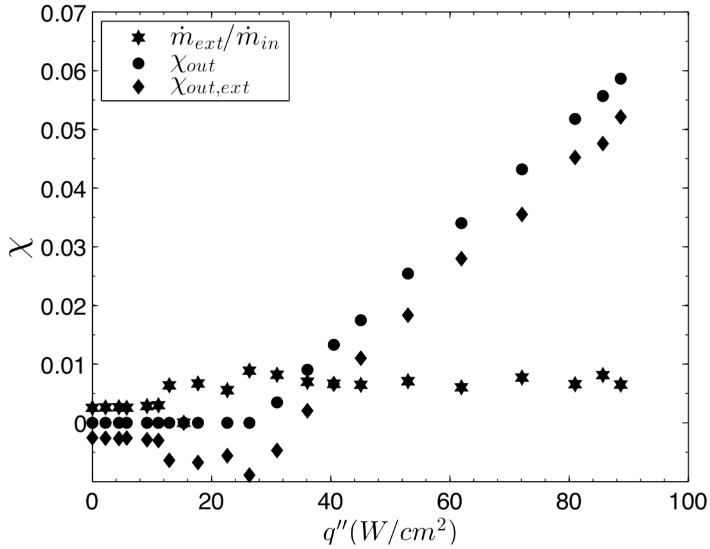

Figure 11 Comparison of extracted mass, exit quality with no extraction, and exit quality with extraction for a Re = 5000, H/d_j =1.5 case presented in Figure 10.

Evident from Figure 11 is that, with vapour extraction, the quality of the water leaving the confined gap is lower than that with no extraction. This phenomenon is observed by comparing the diamonds to the circles, respectively. Shown as stars is the mass of vapour extracted divided by the incoming mass. Given the current porous surface permeability, the extracted mass appears to be limited to 1%. In the present study, removal of vapour tends to enhance heat transfer whereas Chang et al (1995b) found incorporation of vapour to enhance heat transfer. To what degree enhancement does or does occur requires further study and will likely depend heavily on the quality and perhaps on a range of other parameters.

CONCLUSIONS

Heat transfer from a sub-cooled, confined, submerged jet impingement was experimentally examined as a function of jet Reynolds number and non-dimensional gap spacing. The test device consists of a 4 mm diameter jet, a 38 mm diameter gold plated aluminum heater block and a variable gap height. The upper confinement surface, currently impermeable, is replaceable to allow for vapor extraction studies. Distilled and degassed water at 10°C sub-cooling was used as the working fluid. Evaluation of the heat losses allowed for the input power to be corrected and used to calculate the applied surface heat flux. The surface temperature was extrapolated using a 1-D conduction model and temperature readings from thermocouples inside the heater block.

Heat transfer performance was presented using boiling curves, the results of which were compared to existing correlations. Boiling curves indicated that an increase in jet Reynolds number served to enhance the single-phase regime heat transfer and delay the onset of nucleate boiling. Gap height was determined not to influence heat transfer performance over the ranges gap heights tested, in either the single-phase or two-phase flow regimes. Using constants deemed most appropriate for the existing fluid and impingement surface conditions, correlations were used predict measured heat flux within 25% for the two higher Reynolds number cases. The results from the lowest mass flow rate case were outside the 25% error margin for the single-phase and partial nucleate boiling regimes. Because the two-phase component of the correlation used was derived from the Rohsenow (1952) pool boiling correlation, which is only valid for the isolated bubble region of the boiling curve, the correlation over predicts the surface heat flux. This is reflected in the comparison of the correlation to the experimental data at heat fluxes above 75 W/cm^2.

ACKNOWLEDGEMENTS

The authors would like to express their gratitude to Dr. Mark Spencer with the Office of Naval Research for financial support under contract number N000140911079 and to the following students, Adam Damiano, Nick Cappello, Randall Fox and Saran Salijik, for helping in the laboratory and for participating in brainstorming sessions.

NOMENCLATURE

A	Area, m^2
c_p	Specific heat of liquid phase, kJ/kg-K
$C_{s,f}$	Surface fluid parameter
d	Diameter, m
g	Gravitational acceleration, m/s^2
$\bar{h}$	Spatially averaged transfer coefficient, W/m^2-K
H	Gap spacing, m

i Enthalpy, kJ/kg
i_{lv} Enthalpy of vaporization , kJ/kg
I Current, Amps
k Thermal conductivity, W/m-K
$\dot{m}$ Mass flow rate, kg/s
n Exponent of Prantl number
Re Reynolds number
Pr Prandtl number
T Temperature, °C
q'' Heat flux, W/m^2
Q Power, W
V Voltage

Greek Letters
μ Viscosity, kg/m-s
ρ Density, kg/m^3
σ Surface tension, N/m
χ Quality

Subscripts
1Φ Single-phase
Al Aluminum
b Bulk
ext Extraction
HB Heater block
in Inlet
j Jet
l Liquid
$loss$ Experimentally determined losses
NB Nucleate boiling
out Outlet
s Surface
sat Saturation
v Vapor
w Wall

REFERENCES

Chang, C., Kojasoy, G., Landis F., Downing S. (1995a). Confined Single- and Multiple-Jet Impingement Heat Transfer - 1. Turbulent Submerged Liquid Jets, *Int. J. Heat Mass Transfer*, Vol. 38, pp. 833-842.

Chang, C., Kojasoy, G., Landis F., Downing S. (1995b). Confined Single- and Multiple-Jet Impingement Heat Transfer - II. Turbulent Two-Phase Flow, *Int. J. Heat Mass Transfer*, Vol. 38, pp. 833-842.

Figliola. R.S., Beasley, D.E. (1995). *Theory and Design for Mechanical Measurements,* Wiley, New York, NY.

Garimella, S.V., Rice, R.A. (1995). Confined and Submerged Liquid Jet Impingement Heat Transfer, *Journal of Heat Transfer*, Vol. 117, pp. 871-877.

Garimella, S.V., Nenaydykh, B. (1996). Nozzle-Geometry Effects in Liquid Jet Impingement Heat Transfer, *Int. J. Heat Mass Transfer*, Vol. 39, pp. 2915-2923.

Kamata, T., Kumagai, S., Takeyama, T. (1988). Boiling Heat Transfer to an Impinging Jet Spurted into a Narrow Space (Part 1, Space with an Open End), *Heat Transfer - Japanese Research*, Vol. 17, pp. 71-80

Katto, Y., Kunihiro, M. (1973). Study of the Mechanism of Burn-out in Boiling System of High Burn-out Heat Flux, *Bulletin of the JSME*, Vol. 16, pp. 1357-1366.

Li, Y.C., Garimella, S.V. (2001). Prandtl-Number Effects and Generalized Correlations for Confined and Submerged Jet Impingement, *Int. J. Heat Mass Transfer*, Vol. 44, pp. 3471-3480.

Liu, Z., Tong, T., Qiu, Y. (2004). Critical Heat Flux of Steady Boiling for Subcooled Water Jet Impingement on the Flat Stagnation Zone, *Journal of Heat Transfer*, Vol. 126, pp. 179-183.

Ma, C., Bergles, A. (1986). Jet Impingement Nucleate Boiling, *Int. J. Heat Mass Transfer*, Vol. 29, pp. 1095-1101.

Monde, M., Katto, Y. (1978). Study of Burn-Out in a High Heat Flux Boiling System with an Impinging Jet, *Int. J. Heat Mass Transfer* Vol. 21, pp. 295-305.

Mudawar, I. (2001). Assessment of High-Heat-Flux Thermal Management Schemes, *IEEE Transactions on Components and Packaging Technologies*, Vol. 24, pp. 122-141.

Mudawar, I., and Wadsworth, D. (1991). Critical Heat Flux from a Simulated Chip to a Confined Rectangular Impinging Jet of Dielectric Liquid, *Int. J. Heat Mass Transfer*, Vol. 34, pp. 1465-1479.
Pioro, I., (1999). Experimental Evaluation of Constants for the Rohsenow Pool Boiling Correlation, *Int. J. Heat Mass Transfer*, Vol. 42, pp. 2003-2013.
Rohsenow, W. (1952). Method of Correlating Heat-Transfer Data for Surface Boiling of Liquids, *Transactions of ASME*, Vol. 74, pp. 969-976.
Sabo, M. (2012). Performance and Flow Stability Characteristics in Two-Phase Confined Impinging Jets, Master's thesis, Oregon State University, Corvallis, OR.
Stull, C. (2012). Enhancement of Heat Transfer and Flow Stability in a Confined Impinging Jet using In-Situ Vapor Extraction, Master's thesis, Oregon State University, Corvallis, OR. (In progress).
Wadsworth, D., Mudawar, I. (1990). Cooling of a Multichip Electronic Module by Means of Confined Two-Dimensional Jets of Dielectric Liquid, *Journal of Heat Transfer*, Vol. 112, pp. 891-898.
Wolf, D., Incropera, F. P., Viskanta, R. (1993). Jet Impingement Boiling. *Advances in Heat Transfer*. Vol. 23, pp. 1-132,
Zhou, D., Ma, C. (2004), Local Jet Impingement Boiling Heat Transfer with R-113. *Heat and Mass Transfer*, Vol. 40, pp. 539-549.